

# Electron-irradiated $n^+$ -Si as hole injection tunable anode of organic light-emitting diode

Y. Z. Li · Z. L. Wang · Y. Z. Wang ·  
H. Luo · W. J. Xu · G. Z. Ran · G. G. Qin

Received: 11 June 2010/Revised: 30 July 2012/Published online: 23 November 2012  
© Springer-Verlag Berlin Heidelberg 2012

**Abstract** Traditionally, n-type silicon is not regarded as a good anode of organic light emitting diode (OLED) due to the extremely low hole concentration in it; however, when doped with Au element which acts as carrier generation centers, it can be, as shown in our previous work. In this study, we demonstrate a new kind of carrier generation centers in  $n^+$ -type silicon, which are the defects produced by 5 MeV electron irradiation. The density of carrier generation centers in the irradiated  $n^+$ -Si anode can be controlled by tuning the electron irradiation time, and thus hole injection current in the OLEDs with the irradiated  $n^+$ -Si anode can be optimized, leading to their much higher maximum efficiencies than those of the OLEDs with non-irradiated  $n^+$ -Si anode. For a green phosphorescent OLED with the irradiated  $n^+$ -Si anode, the current efficiency and power efficiency reach up to 12.1 cd/A and 4.2 lm/W, respectively.

## 1 Introduction

An efficient silicon light source plays a key role in silicon optoelectronics. Long-term intensive efforts have been

made on this topic. A promising route being investigated is to combine the excellent electroluminescence (EL) ability of organic semiconductors with the highly mature technology of silicon materials [1–12]. In an organic light emitting diode (OLED), n-type silicon, just like p-type silicon, could be used as an anode in principle because it also has a high work function [13]; however, the EL efficiency of the n-Si anode OLEDs is usually much lower than that of the p-Si anode counterparts. Recently, by introducing Au generation centers into the bulk  $n^+$ -Si anodes, the EL efficiency has been improved greatly to the same level of the p-Si anode counterparts for both fluorescent and phosphorescent emitters [14, 15]. Unfavorably, Au is a fast-diffusing element in silicon and usually considered contaminant in silicon electronic processes [16]. So it is necessary to search to find a new kind of hole generation centers as substitution. Here, we introduce the defects in n-type silicon produced by 5 MeV electron irradiation as hole generation centers. Their density can be controlled by tuning the irradiation time [17, 18] and thus the hole injection can be optimized. After such optimization, the phosphorescent OLED with irradiated  $n^+$ -Si anode achieves a maximum current efficiency of 12.1 cd/A and a maximum power efficiency of 4.2 lm/W; and the fluorescent OLED with such an anode reaches 1.0 cd/A and 0.2 lm/W, respectively, which are close to those of the ITO anode OLEDs reported. The electron irradiated  $n^+$ -Si should be more compatible to Si-based optoelectronic integration compared to the counterpart with fast diffusing metallic elements.

## 2 Experiments

The used  $n^+$ -type silicon wafers are (100) oriented and have an electrical resistivity of about 0.01  $\Omega$  cm. They

---

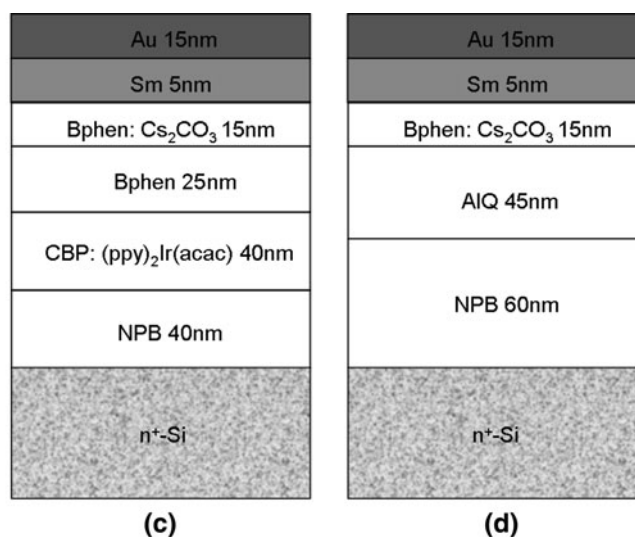
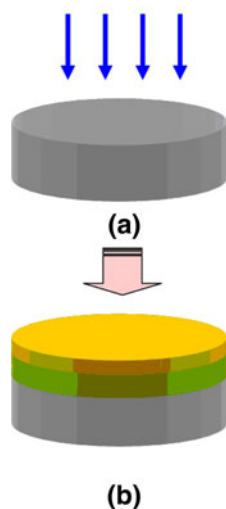
Y. Z. Li (✉) · Z. L. Wang · Y. Z. Wang · H. Luo ·  
W. J. Xu · G. Z. Ran · G. G. Qin  
State Key Lab for Mesoscopic Physics,  
School of Physics, Peking University,  
Beijing 100871, China  
e-mail: liyanzhao\_1983@163.com

G. Z. Ran  
e-mail: rangz@pku.edu.cn

G. G. Qin  
e-mail: qingg@pku.edu.cn

G. G. Qin  
Key Lab of Semiconductor Materials,  
CAS, Beijing 100083, China

**Fig. 1** **a** An  $n^+$ -Si wafer is irradiated by 5 MeV electrons, **b** deposition of the organic and cathode metal layers on the electron irradiated  $n^+$ -Si wafer; the schematic structures of **c** phosphorescent and **d** fluorescent OLEDs with the irradiated  $n^+$ -Si anode



were first rinsed in a 2 % HF solution for 4 min to etch off the native oxide film and then routinely cleaned. The cleaned wafers were irradiated by the 5 MeV electrons for a series of durations of 2, 4, 8, 16 and 32 min in the atmosphere with a dose rate of  $1.6 \times 10^{12} \text{ cm}^{-2} \text{ s}^{-1}$  in a BF-5 electron linac, as illustrated in Fig. 1a. To verify the formation of generation centers caused by electron irradiation, some of the irradiated  $n^+$ -Si samples were annealed at the temperature of 100 or 200 °C for 10 min in a  $\text{N}_2$  atmosphere. The organic materials and the cathode metals were thermally evaporated successively on the treated  $n^+$ -Si wafers, as illustrated in Fig. 1b. The typical deposition rate was  $\sim 1 \text{ \AA/s}$  monitored by quartz crystal oscillators. The HTL is *N,N'*-bis-(1-naphthyl)-diphenyl-1, 1'-biphenyl-4,4'-diamine (NPB). For the phosphorescent OLED, the emitter is bis (2-phenylpyridine) iridium (III) acetylacetonate [(ppy)<sub>2</sub>Ir(acac)], which is doped into the host material, 4,4'-*N,N'*-dicarbazole-biphenyl (CBP). The most part of the electron transport layer (ETL) is 4,7-diphenyl-1, 10-phenanthroline (BPhen), and another 15 nm Bphen is doped by  $\text{Cs}_2\text{CO}_3$  (mass ratio 1:1) as the electron injection layer and the another part of the ETL. The cathodes are stacked Sm/Au bilayers. For the fluorescent OLED, tris-(8-hydroxyquinolino) aluminium (AlQ) is the emitter and a part of the ETL. The resulting phosphorescent devices have a structure of irradiated  $n^+$ -Si/NPB 40 nm/CBP: (ppy)<sub>2</sub>Ir(acac) ( $\sim 10 \text{ wt } \%$ ) 40 nm/Bphen 25 nm/Bphen:  $\text{Cs}_2\text{CO}_3$  15 nm/Sm 5 nm/Au 15 nm, as shown in Fig. 1c. The fluorescent devices have a similar structure as shown in Fig. 1d. Spectra and luminance of the OLEDs were measured in atmosphere by a PR705 spectrometer. Current–voltage characteristics were measured by a computer-controlled Keithley 2400 source meter.

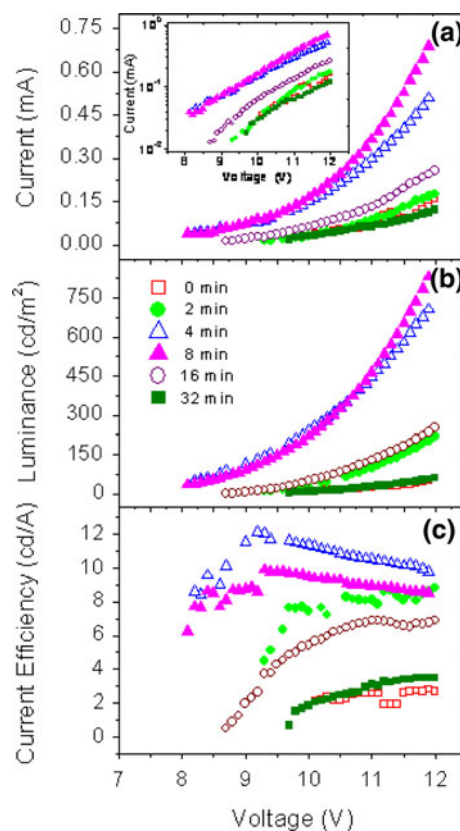
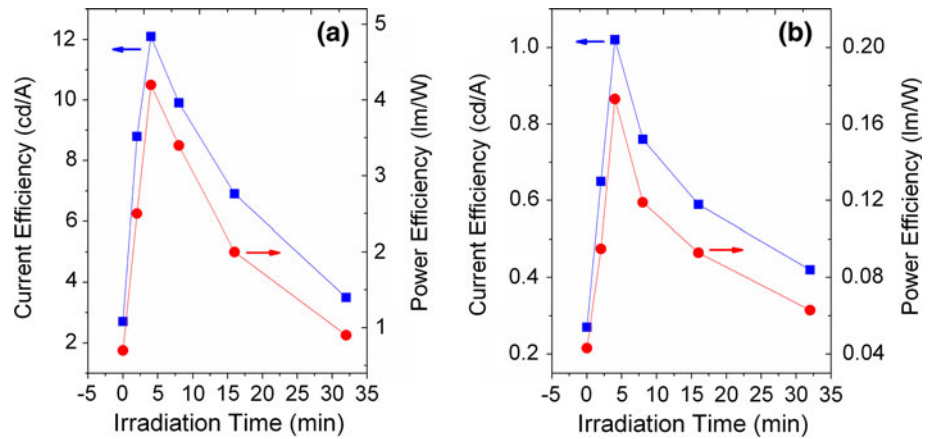


**Fig. 2** The characteristics of **a** current–voltage, **b** luminance–voltage, and **c** current efficiency–voltage for the phosphorescent OLEDs with the irradiated  $n^+$ -Si anode for a series of irradiation times. The inset of **a** depicts the current–voltage characteristics in semi-logarithmic coordinates

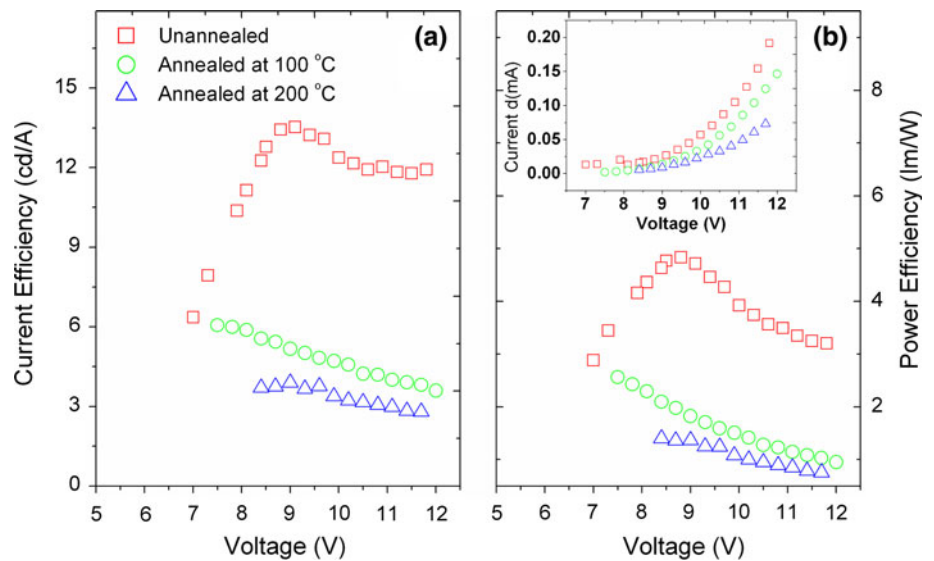
### 3 Results and discussion

Figure 2 shows the current–, luminance– and current efficiency–voltage curves of the phosphorescent OLEDs with

**Fig. 3** The characteristics of current efficiency and power efficiency with the irradiation time for **a** phosphorescent and **b** fluorescent OLEDs with the irradiated n<sup>+</sup>-Si anode



**Fig. 4** The characteristics of a current efficiency–voltage and b power efficiency–voltage for the OLEDs with the 4 min irradiated and 100, 200 °C or unannealed n<sup>+</sup>-Si anodes. The inset in b shows the current–voltage characteristics for the OLEDs indicated in this figure



the irradiated n<sup>+</sup>-Si anodes. The inset of Fig. 2a depicts the current–voltage characteristics in semi-logarithm coordinates. With the irradiation time increase, the currents and luminance at a same voltage increase first and then decrease as shown in Fig. 2a, b. The best irradiation time is 4 min. The OLED with the non-irradiated n<sup>+</sup>-Si anode has the lowest current and luminance as expected because of its lowest hole injection. When n<sup>+</sup>-Si/HTL is reverse biased, some of the defects produced by electron irradiation can emit holes into the valence of the silicon and these holes are then injected into the HTL under the electrical field. With the increase of the irradiation time, the generation center density increases and so does the hole injection from anode to HTL. At first, the increase of the hole injection results in the improvements of hole–electron balance, the current, then luminance and finally the efficiency. However, if the irradiation time is very long, the hole injection increases to be greater than the electron injection; so both the luminance and the efficiencies drop. For example, when the irradiation time is 0 and 32 min, the maximum current

efficiencies of the two devices are only 2.7 and 3.5 cd/A as shown in Fig. 2c, respectively. As summarized in Fig. 3, the current efficiency and power efficiency increase first and then decrease with the increase of irradiation time for both the phosphorescent (Fig. 3a) and fluorescent (Fig. 3b) OLEDs with irradiated n<sup>+</sup>-Si anodes. The best irradiation time is 4 min. For the phosphorescent device, the maximum current efficiency and power efficiency are 12.1 cd/A and 4.2 lm/W, respectively, as shown in Fig. 3a; for the fluorescent device, they are 1.02 cd/A and 0.17 lm/W, respectively, as shown in Fig. 3b.

To further verify the hole injection enhancement from the electron irradiation, we have studied the annealing effect of the irradiated n<sup>+</sup>-Si anode on the performance of the phosphorescent OLEDs. In the 4 min irradiation case shown in Fig. 4, the higher the annealing temperature, the lower the current. Currents for the two annealed devices are both smaller than that for the unannealed one. The current efficiency (Fig. 4a) and power efficiency (Fig. 4b) follow the evolution trends of the current–voltage curves.

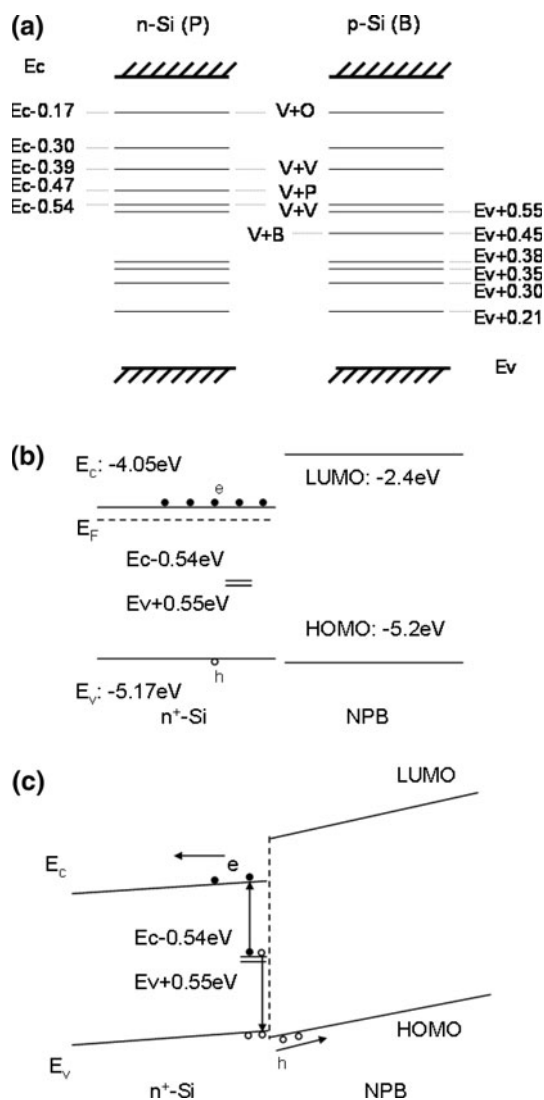


**Fig. 5** **a** The deep-level defects produced in silicon under low-energy electron irradiation, **b** the energy level-alignment scheme at zero bias, **c** the process scheme of hole generation and injection from  $n^+$ -Si anode into the NPB layer

Compared to the irradiated but non-annealed  $n^+$ -Si, the generation center density becomes lower in the irradiated and annealed  $n^+$ -Si anode. When annealed above 200 °C, the effective generation centers almost vanish [19]. Thus, the hole injection from the irradiated and annealed  $n^+$ -Si anode into the HTL will be less than electron injection again at a reverse bias for the  $n^+$ -Si/HTL junction, causing the decrease of the current efficiency. For the phosphorescent OLEDs with the irradiated and 100 °C-annealed  $n^+$ -Si anode, the highest current efficiency and power efficiency reduce to 6.1 cd/A and 2.6 lm/W, respectively, and at the annealing temperature of 200 °C, they reduce further to only 3.9 cd/A and 1.5 lm/W, respectively, close to those of the non-irradiated counterpart.

Figure 5a shows a series of deep-level defects produced in  $n^+$ -type silicon under the low-energy electron irradiation [20, 21]. Some of them are in close proximity to the middle of the silicon band gap, such as the level of  $E_c - 0.54$  eV and the one of  $E_v + 0.55$  eV, and they will play a role of generation centers just like Au center in silicon reported in Ref. [14]. Figure 5b shows a scheme of energy level alignment at zero bias. The top of the silicon valence band is very close to the highest occupied molecular orbits (HOMOs) of NPB. Figure 5c illustrates that holes are emitted from the levels of the generation centers into the silicon valence band and then injected into the HOMOs of NPB under the forward electric field. The other levels, much farther from the silicon valence band or conduction band than these middle levels, can hardly emit electrons into silicon conduction band and hardly emit holes into the silicon valence band, i.e., they are not effective hole generators.

## 4 Conclusion

We successfully utilized the defects in  $n^+$ -Si produced by 5 MeV electron irradiation as hole generation centers instead of Au. At the irradiation time of 4 min, the current efficiency and power efficiency of the phosphorescent OLEDs with irradiated  $n^+$ -Si anode reach the maximum values of 12.1 cd/A and of 4.2 lm/W, respectively; for the fluorescent devices, they are of 1.02 cd/A and of 0.17 lm/W, respectively. All efficiencies are evidently higher than those of the counterparts with non-irradiated  $n^+$ -Si anode. The OLEDs with irradiated and annealed  $n^+$ -Si anode show lower efficiencies compared to the unannealed one, which indicates the vanishing of generation center in the annealing process.

**Acknowledgments** This work is supported by the National Natural Science Foundation of China (Grant No. 11174018; 61176041) and the National 863 Project (Grant No. 2012AA012203).

## References

1. I.D. Parker, H.H. Kim, Appl. Phys. Lett. **64**, 1774 (1994)
2. H.H. Kim, T.M. Miller, E.H. Westerwick, Y.O. Kim, E.W. Kwock, M.D. Morris, M. Cerullo, J. Lightwave Technol. **12**, 2107 (1994)
3. W. Lek Ng, M.A. Lourenco, R.M. Gwilliam, S. Ledain, G. Shao, K.P. Homewood, Nature **410**, 192–194 (2001)
4. X. Zhou, J. He, L.S. Liao, M. Lu, Z.H. Xiong, X.M. Ding, X.Y. Hou, F.G. Tao, C.E. Zhou, S.T. Lee, Appl. Phys. Lett. **74**, 609 (1999)
5. G.G. Qin, A.G. Xu, G.L. Ma, G.Z. Ran, Y.P. Qiao, B.R. Zhang, W.X. Chen, S.K. Wu, Appl. Phys. Lett. **85**, 5406 (2004)
6. G.Z. Ran, Y.H. Xu, G.L. Ma, A.G. Xu, Y.P. Qiao, W.X. Chen, G.G. Qin, Semicond. Sci. Technol. **20**, 761 (2005)

7. X.L. Zhu, J.X. Sun, H.J. Peng, Z.G. Meng, M. Wong, H.S. Kwok, *Appl. Phys. Lett.* **87**, 083504 (2005)
8. C.J. Huang, S. Han, D. Grozea, A. Turak, Z.H. Lu, *J. Appl. Phys.* **97**, 86107 (2005)
9. L. Yang, Z.G. Meng, C.Y. Wu, W. Man, K.S. Hoi, S.Z. Xiong, *Light-emitting Diode Mater. Devices* **II**(6828), J8280 (2008)
10. S.M. Chen, Y.B. Yuan, J.R. Lian, X. Zhou, *Opt. Express* **15**, 14644–14649 (2007)
11. R.J. Curry, W.P. Gillin, A.P. Knights, R. Gwilliam, *Appl. Phys. Lett.* **77**, 2271 (2000)
12. W.Q. Zhao, G.Z. Ran, Z.W. Liu, Z.Q. Bian, K. Sun, W.J. Xu, C.H. Huang, G.G. Qin, *Opt. Express* **16**, 5158–5163 (2008)
13. P. Ball, *Nature* **409**, 974–976 (2001)
14. Y.Z. Li, G.Z. Ran, W.Q. Zhao, G.G. Qin, *J. Phys. D Appl. Phys.* **41**, 155107 (2008)
15. Y.Z. Li, G.Z. Ran, W.Q. Zhao, G.G. Qin, *Jpn. J. Appl. Phys.* **47**, 8579 (2008)
16. R.H. Wu, A.R. Peaker, *Solid-State Electron* **25**, 643 (1982)
17. J.R. Srouf, C.J. Marshall, P.W. Marshall, *IEEE Trans. Nucl. Sci.* **50**, 653–669 (2003)
18. T. Wada, K. Yasuda, S. Ikuta, M. Takeda, H. Masuda, *J. Appl. Phys.* **48**, 2145–2152 (1977)
19. H.J. Stein, F.L. Vook, *Phys. Rev.* **160**, 790 (1967)
20. J.W. Walker, C.T. Sah, *Phys. Rev. B* **7**, 4587 (1973)
21. T.W.K. Yasuda, S. Ikuta, M. Takeda, H. Masuda, *J. Appl. Phys.* **48**, 2145 (1977)